ANL/NE-17/3

Argonne NATIONAL LABORATORY

Low-Cost, High-Performance Alternatives for Target Temperature Monitoring Using the Near-Infrared Spectrum

Nuclear Engineering Division

ANL/NE-17/3

Low-Cost, High-Performance Alternatives for Target Temperature Monitoring Using the Near-Infrared Spectrum

by
Matt Virgo, Kevin J. Quigley, Sergey Chemerisov, and George F. Vandegrift
Nuclear Engineering Division, Argonne National Laboratory

February 2017

CONTENTS

FIGURES

FIGURES (Cont.)

LOW-COST, HIGH-PERFORMANCE ALTERNATIVES FOR TARGET TEMPERATURE MONITORING USING THE NEAR-INFRARED SPECTRUM

ABSTRACT

A process is being developed for commercial production of the medical isotope Mo-99 through a photo-nuclear reaction on a Mo-100 target using a high-power electron accelerator. This process requires temperature monitoring of the window through which a high-current electron beam is transmitted to the target. For this purpose, we evaluated two near infrared technologies: the OMEGA Engineering iR2 pyrometer and the Ocean Optics Maya2000 spectrometer with infrared-enhanced charge-coupled device (CCD) sensor. Measuring in the near infrared spectrum, in contrast to the long-wavelength infrared spectrum, offers a few immediate advantages: (1) ordinary glass or quartz optical elements can be used; (2) alignment can be performed without heating the target; and (3) emissivity corrections to temperature are typically less than 10%. If spatial resolution is not required, the infrared pyrometer is attractive because of its accuracy, low cost, and simplicity. If spatial resolution is required, we make recommendations for near-infrared imaging based on our data augmented by calculations

1 INTRODUCTION

NorthStar Medical Technologies is pursuing production of the medical isotope Mo-99 through a photo-nuclear reaction on Mo-100 using a high-power electron accelerator. To make this pathway for Mo-99 production commercially feasible, enriched Mo-100 material is used for the target. The cost of the Mo-100 is in the range of $500-1000/g for kilogram quantities. The high cost of the target material and the desire to maximize production drive the requirement to minimize the size of the target and maximize the power deposition on the target. High power deposition in the target requires an unconventional cooling solution.

Argonne National Laboratory (Argonne) and Los Alamos National Laboratory (LANL) have demonstrated gaseous helium cooling of the metal molybdenum target at high power densities. This method of cooling requires high flow and high pressure of the helium gas [1–4]. The target window [5,6] separates the high-pressure helium gas inside the target from the vacuum inside the accelerator beamline; this pressure differential introduces significant stress on the window. Also, the high-current electron beam transmitting through the window deposits significant power into the window material. The window is cooled by gaseous helium only on one side, which makes the window the most stressed component of the target. To ensure the integrity of the window is not compromised, continuous temperature monitoring is required.

In our earlier production and thermal tests [7-9], this function was carried out with a FLIR A655sc thermal imaging camera. The A655sc uses a microbolometer array sensitive in the 7.4–14 μm wavelength range. Unfortunately, it exhibited limited lifetime in the high radiation environment of the accelerator area. The purpose of the study reported here was to evaluate potentially more robust near infrared technologies (for this purpose, defined as the approximate wavelength range of 0.8– 2.0 μm) as alternatives to the microbolometer based approach with an emphasis on low cost, adequate resolution, reliability, and practicality.

1.1 INFRARED TEMPERATURE MEASUREMENT

Any material body emits thermal radiation whose characteristics are determined primarily by its temperature, and only to a lesser degree by its specific properties. This phenomenon is the basis for the technique of infrared thermometry. In applications where direct physical contact with an object is not possible or desirable, infrared thermometry is the primary temperature measurement method applicable. Because metals lose their strength at higher temperatures, our method of gaseous helium cooling requires temperature monitoring of the window, which will have high pressure He gas on one side and a vacuum on the other. Thermometry in the infrared spectrum should be considered as an appropriate technique for monitoring target window temperature.

A hypothetical material with perfect radiative properties, known as a black body, has a radiation spectrum determined by Planck’s law,

$$L(\lambda, T) = \frac{2hc^2}{\lambda^5} \frac{1}{e^{\frac{hc}{\lambda kT}} - 1},$$

where *h* is Planck's constant, *c* is the velocity of light, λ is the radiation wavelength, *k* is Boltzmann's constant, and *T* is the temperature of the body in absolute temperature units. In this report, except where noted, macroscopic quantities are given in MKS units. In the MKS system, length is measured in meters (m), time is measured in seconds (s), velocity is measured in m/s, energy is measured Joules (J), power is measured in watts (W), and temperature is measured in the Kelvin scale. Planck's constant has units of J · s, and Boltzmann's constant has units of J/K. For microscopic energies, units of electron volts (eV) are used. A photon with an energy of 1 eV has a wavelength of 1.25 μm, which is in the near infrared region. At 25°C (room temperature), $kT = 26$ meV. In the MKS system, the spectral radiance *L* (differential in wavelength) is in units of $\mathrm{W{\cdot}m^{-3} \cdot sr^{-1}}$. The black body spectra corresponding to several specific temperatures are shown in Figure 1.

As can be seen, the spectra exhibit a strong temperature dependence. The peak of the spectra shifts to shorter wavelengths as the temperature increases. Specifically, the peak of the distribution occurs at a photon energy of approximately 5 kT. In reference to the figure, this corresponds to a wavelength of $hc/5kT$. The intensity at the peak increases proportionally to T^5. Also, by the Stefan-Boltzmann law, the total radiated power increases proportionally to T^4. As a result, the temperature can be determined by measuring the spectrum at specific wavelengths or by measuring the total power radiated. In addition, when material-specific properties that affect the absolute magnitude of the spectra are considered, one can determine the temperature by looking at the shape of the spectrum. Typically, this entails determining the ratio of the power radiated at two wavelengths, a technique termed two-wavelength, two-color, or ratio thermometry/pyrometry.

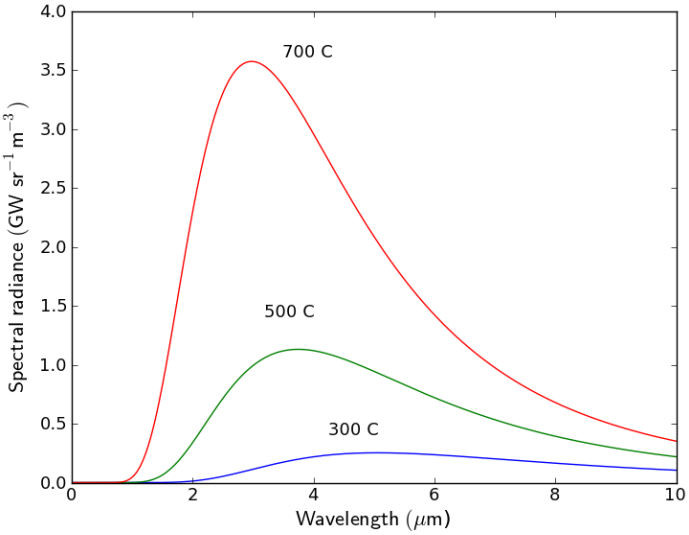

FIGURE 1 Blackbody spectra for three temperatures relevant to target window temperature monitoring.

For wavelengths near and below the peak, the Wien approximation to Planck's law can be used. In the Wien approximation, $L(\lambda, T) = (2hc^2/\lambda^5)e^{-hc/\lambda kT}$.

For single-wavelength measurements, a simple analysis can be used to determine which wavelengths are most suited for measuring a given temperature. The minimum discernable change in detector signal is given by the noise *N*, which can be measured, for example, in detector counts. For a given detector, if the exposure time is kept constant, the noise will be constant. The slope of the black body distribution relates uncertainty in optical intensity to uncertainty in temperature. In the Wien approximation, the relationship between change in detector signal and change in temperature is simply $dL/dT = hc/\lambda kT$, or equivalently $dT/T = (\lambda kT/hc)\ dL/L$. Physically, $\lambda kT/hc$ is the dimensionless ratio of the energy *kT* to the photon energy. Since *L* is linearly related to the number of detector counts *Q* by a constant factor determined by the light collection efficiency, $dQ/Q = dL/L$. Approximately, then, the temperature resolution $\Delta T_{\text{min}}/T = (\lambda kT/hc)\ \Delta Q_{\text{min}}/Q$.

As an example, consider a detector sensitive at 1.23 μm (1 eV) that records an average of 50 dark counts per exposure. The noise is then $\sqrt{50} \approx 7$ counts [10]. At 600°C, $kT = 75$ meV, so $\lambda kT/hc$ is 0.075. To measure a relative temperature rise $\Delta T_{\text{min}}/T$ of 1% (6° C), the nominal signal must be at least $7 \times .075/.01 = 53$ counts per exposure. This corresponds to an extremely weak signal. For context, a CCD pixel typically saturates at 10^5–10^6 counts [11]. In other words, a strong signal is not needed if there is no requirement of high temperature resolution. Critically, this application requires consideration of the effect of the high radiation field on the dark signal.

As discussed below, real objects emit less energy than black bodies. The ratio of actual to theoretical power radiated is called the "emissivity." The ability to make accurate temperature measurements by the single-color method is limited by the accuracy with which the emissivity is known. To an extent, this limitation can be sidestepped with the two-color method. The accuracy of the two-color method is determined by the ratio of the emissivities at the two wavelengths, and the emissivity often does not change dramatically over limited wavelength ranges. Likewise, if the surface of the target window is modified or damaged during operation, a two-color measurement is less likely to be affected than a single-color one. Furthermore, if the optics in the pyrometer darken due to radiation damage, the two-color measurement will not be affected as long as the change is not strongly wavelength dependent. The downside of the two-color method is that the sensitivity to temperature change is reduced relative to the single-color method, with $dT/T = -kT/(hc/\lambda_1 - hc/\lambda_2)\ dr/r$, where r is the ratio of the emissivities. As a consequence, the required temperature resolution must be considered when selecting the wavelengths. Specifically, the wavelengths must not be too close together.

In some cases, two-color methods offer the advantage of being able to measure the temperature of the hottest region of an unevenly heated surface [12]. If this is the case, spatial resolution requirements can be relaxed. The basis for the technique is that the dependence of emitted power on temperature is wavelength dependent. This works particularly well when the temperature differential between the hot spots and the reaming surface is large. In that case, the contribution from the cooler areas can be neglected, and it becomes possible to use the two data points to determine whether an increase in radiated power is due to a large patch at slightly

elevated temperature or a small patch at more severely elevated temperature. Still, a two-color measurement is more strongly weighted toward hot spots than a single-color measurement, and even a single-color measurement provides some weighting.

As a general point of reference, note that by the Stefan-Boltzmann law, the surface of the filament of a typical incandescent light bulb, which operates around 2100°C, emits $((2100 + 273)/(500 + 273))^4 = 89$ times more power than it would at 500°C. Though the power is significantly lower, it would still not be a challenge to detect (with an infrared detector), even at considerable distance.

1.2 EMISSIVITY CORRECTION

The emission distributions described above are for the case of an ideal radiator. They define the maximum power that can be radiated at a given wavelength by an object at a given temperature. Real objects radiate less power. The ratio of power radiated by a real object to power radiated by a similar black body is called "emissivity." When making temperature measurements, the measured power must be corrected for the emissivity of the object. Given a raw temperature measurement T_r made near the wavelength λ, the actual temperature T_a of a surface with emissivity ε is $T_a/T_r = 1 + (-\ln \varepsilon)\, \lambda k T_a/hc$. Most materials have an emissivity that falls between 0.1 and 1.0 [13], though metals with a mirror-like surface can have emissivities below 0.1. Surface finish and the presence or absence of oxidation are two major factors that can modify a material's emissivity. Generally, though, the emissivity correction is not large for this wavelength and temperature range, where the photon energy hc/λ is on the order of 1 eV and kT is on the order of 100 meV. Since $(-\ln \varepsilon) = 1$ when $\varepsilon = 0.37$, the correction is expected to be no larger than about 10% under the given conditions.

The most accurate method for determining the emissivity correction is to calibrate the infrared measurement against an alternative measurement technique under conditions matching, as closely as possible, the desired operating environment. A typical approach would be to use a contact probe such as a thermocouple. In cases where this is not practical, the emissivity can be approximated based on the properties of the material. Also, if the emissivity is known, or assumed to be, constant across a given wavelength range, the temperature can be determined by the two-color method described above.

1.3 DETECTOR OPTIONS

A number of materials can be used as photodetectors in the infrared spectrum [14]. However, for wavelengths longer than about 2.5 μm, dark current becomes too high for the devices to operate unless they are actively cooled below room temperature. This added requirement greatly increases the cost and complexity of the detector. Silicon detectors, which are ubiquitous and inexpensive, have a long wavelength limit between 1.1 and 1.2 μm. Uncooled indium gallium arsenide (InGaAs) detectors of high sensitivity can be designed to detect photons out to 1.6 μm. The range of room-temperature InGaAs detectors can be extended to about 2.6 μm, but the sensitivity falls rapidly. Beyond that range, the only common uncooled, infrared

sensitive detector array is the microbolometer, a true thermal detector sensitive in the 7.5–14 μm band. The microbolometer has an FLIR A655sc camera that has been used in the previous production and thermal tests cited above. Drawbacks of the microbolometer-based detector for this application are its low sensitivity and apparent susceptibility of the electronics to radiation damage.

2 EXPERIMENTAL

2.1 LIGHT COLLECTION

The lens that was used in the experiments described herein, in combination with the pyrometer or spectrometer, has a specified field of view of $\alpha = 2.3°$. The fiber provided has a core diameter of $d = 1000$ µm. By the relationship $\alpha = 2\tan^{-1} d/2f$, the focal length f of the lens is approximately 25 mm. The diameter of the lens (*D*) is approximately 8 mm, implying the f-number (f/D) is f/3. The corresponding numerical aperture $\left[\text{NA} = 1/\left(2 \times \text{f-number}\right)\right]$ equals 0.17. The numerical aperture of the fiber is not given, but typically, inexpensive glass fibers have an NA of approximately 0.2, so it is likely that all the light collected by the lens is accepted by the fiber. The spectrometer is specified to be f/4, so $(3/4)^2 = 56\%$ of the collected light is accepted by the spectrometer.

In these experiments, the lens was placed 20 cm from the target. Given the 2.3° field of view, this implies light is collected over an 8-mm diameter spot. In a production facility, it would be necessary to move the optics back about 3 m from the target to allow for radiation shielding. If a similar spot size were imaged onto a similar-sized optical fiber, the light collection would be $(20\ \text{cm}/3\ \text{m})^2 = 0.0044$, or 225 times lower. If the diameter of the lens aperture were increased from 8 mm to 25 m, the reduction would be mitigated by a factor of $(25/8)^2 = 10$, resulting in a net efficiency about 22 times lower. A more complete analysis of light collection requirements is given in the conclusion section. Generally speaking, for the temperatures being considered, light collection does not present a challenge at the longer end of the practical wavelength range but becomes an issue for wavelengths close to the visible spectrum.

The spectrometer we used covers the shorter wavelength range. The pyrometer covers the long wavelengths for single-wavelength measurements and the whole range for two-color measurements. The specifications, such as temperature resolution, for the pyrometer are specific to the properties of the included lens, so it is not possible to quantify how the resolution would be affected by using a longer lens (which would be needed to image the same spot size at the greater distance), but our calculations indicate that the light collection would be more than sufficient.

2.2 INSTRUMENTS

Two instruments were used in the experiments. The first was the OMEGA Engineering iR2, a single- and dual-wavelength infrared pyrometer [15]. The second was the Ocean Optics Maya2000 spectrometer with a near-infrared enhanced sensor [16]. Photographs of both instruments are shown in Figure 2. This spectrometer covers the 850–1150 nm wavelength range. The test setup consisted of a stainless steel block embedded with heaters and instrumented with thermocouples, isolated in a vacuum chamber.

FIGURE 2 Instruments used in experiments: the OMEGA Engineering IR2c infrared pyrometer and Ocean Optics NIR enhanced Maya200 Pro spectrometer.

2.2.1 OMEGA Engineering iR2

The OMEGA Engineering iR2 is an infrared pyrometer targeted toward industrial temperature monitoring. The model we acquired (-300 option) has a temperature range of 300–1300°C in the single-color mode and 450–1300°C in dual-color mode. (In dual-color mode, at the low end of the temperature range, our measurement results proved inconsistent.) The specified accuracy is 2°C (though this would apply only if the material's emissivity were known in advance with sufficient accuracy.) The specified repeatability is 2°C, and resolution is 1°C. In the specifications, the wavelength span of the detector is given as 0.8–1.7 µm; however, a company representative stated the device has two detectors: one with two silicon sensors covering the high temperature range, and one with a silicon sensor and an indium gallium arsenide (InGaAs) sensor covering the low temperature range. He gave the spectral responses as "typically" 400–1000 nm for the silicon sensor and 1000 nm to about 1600 nm for the InGaAs sensor. In single-color mode, he said the InGaAs sensor is used for the low temperature range (this is the main mode we used). A lens assembly, coupled to the device with an optical fiber, is provided as an accessory. The lens has a 2.3° field of view and a focus variable in the range of 0.2–4 m. The device additionally has temperature control capabilities that were not used in these experiments.

2.2.2 Ocean Optics Maya2000

The Ocean Optics Maya2000, with a near-infrared enhanced sensor, is a fiber-coupled, USB-controlled Czerny-Turner spectrometer. It uses an uncooled, infrared-enhanced CCD sensor manufactured by Hamamatsu Photonics, sensitive to approximately 1200 nm. A 760 nm long-pass filter blocks light from the visible spectrum. The resolution is specified to be approximately 0.82 nm. The integration time for a single measurement can be set in the range of 7.2 ms to 5 s. The signal-to-noise ratio is specified to be approximately 450:1 at full signal,

which we take to mean the condition where the device is nearly saturated at the shortest integration time. The lens assembly provided with the iR2 was also used with the spectrometer.

The spectrometer produced data in one of two formats. First, it could provide the raw number of counts sensed by the detector. Second, it could scale the results relative to a known black body spectrum. For relative measurements, an Ocean Optics HL-2000 tungsten halogen lamp was used as the reference. The temperature of the lamp is 2530°C. For longer integration times, neutral density filters were used to avoid saturating the detector. At the longest integration times, the available filters were not sufficient, and it was necessary to add extra space between the lamp and the entrance of the fiber. In these cases, care was taken to align the face of the fiber to the axis of the lamp; however, some error may have been introduced when this procedure was used. Once a reference spectrum is collected, the response is flattened by reference to the theoretical spectrum. For these experiments, the dynamic range of the optical power was extremely large, so it was necessary to change the integration time depending on the target temperature. As a result, a new reference spectrum had to be acquired for each temperature level.

2.3 CALIBRATION OF INFRARED MEASUREMENTS

To reference the infrared measurements to direct thermocouple measurements, a heater block was machined from 300 series stainless steel. Heating was provided by four 80-W cylindrical cartridge heaters (diameter: 1/4 in.; length: 1 in.; McMaster Carr part number: 3618K421) inserted through holes in the block. A variable autotransformer ("VARIAC") connected to 120 V line voltage provided AC power to the heaters. For direct temperature measurement, two type-K thermocouples were pinned to the block using set screws. One was inserted into a hole near the center of the block, while the other was inserted into a shallow hole near one edge. In practice, the thermocouple near the edge reported significantly lower temperature than all the other measurements, and the measured temperature would often drop and recover during heating to higher temperatures. This behavior could be attributable to poor contact between the thermocouple and the surface. As a result, data collected from this thermocouple were not used.

2.4 VACUUM SYSTEM FOR TEMPERATURE MEASUREMENT

The vacuum system used for temperature measurement is shown in Figure 3. Potted cartridge heaters were inserted into four holes drilled through a stainless steel block, which was mounted within a 6-in. vacuum cross. Two thermocouples were used to monitor the temperature of the block. A vacuum gauge (blue) was installed at the top of the cross to monitor the pressure in the system. At the bottom, the vacuum pump can be seen. Figure 3 shows an image of the heater block at 600°C. Color accuracy of the photograph is not perfect, but the block should be dull red at this temperature [17]. Instead, it is cherry red or orange, implying a temperature in the range of 800–1100°C. Reflection of light from the heaters off the chamber walls likely explains the discrepancy. Direct light from the edges of the heaters is visible on either side of the block.

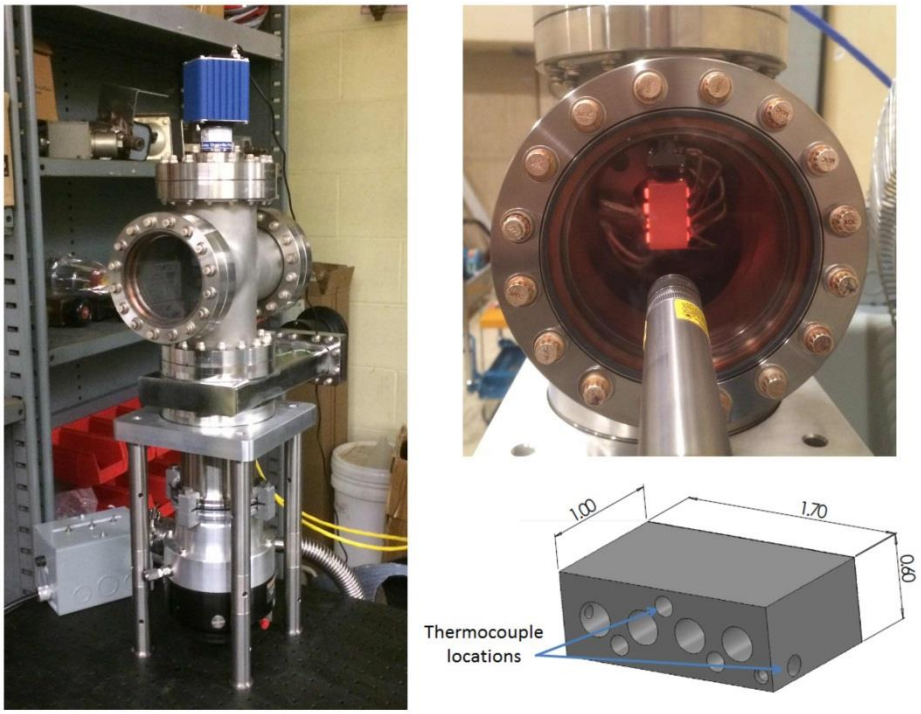

FIGURE 3 Vacuum system used for temperature measurement. Dimensions are in inches. Heater block, heated to 600°C, is shown in top right. Dimensions of heater block given in bottom right.

2.5 DATA COLLECTION

Temperature measurements were collected for the OMEGA Engineering iR2 and Ocean Optics Maya2000. Because of the way the target was designed, it was not possible to properly evaluate the spectrometer for the temperature range of interest. As the experiment was configured, light emitted from the heaters could be reflected off the walls of the chamber onto the target. At shorter wavelengths, the light from the heaters was bright enough relative to the light from the target that the reflected light was sufficiently intense to wash out the direct emission. Although this issue prevented a comprehensive evaluation of this specific spectrometer, the data collected were sufficient to analyze the technique.

3 RESULTS

3.1 INFRARED PYROMETER

Data obtained using the iR2 pyrometer in single-color mode are shown in Figure 4. The lens assembly included with the instrument was used to collect the light. The lens was positioned approximately 0.2 m from the face of the target. The temperature given by the instrument, without emissivity correction, is compared to the thermocouple measurement in the left-hand plot. The emissivity implied by the ratio of the measurements is shown in the plot on the right.

Because the sensor is sensitive to a wide range of wavelengths, it is necessary to account for the shape of the spectral distribution when calculating the implied emissivity. Also, there is no way to determine any possible dependency of the emissivity on wavelength from the available data. Therefore, we assume the emissivity is constant across the wavelength range, which is a reasonable assumption based on the typical characteristics of metals in the near infrared spectrum. With this assumption, the emissivity is given by the ratio of the measured radiated power to the corresponding power that would be radiated by a blackbody at the temperature

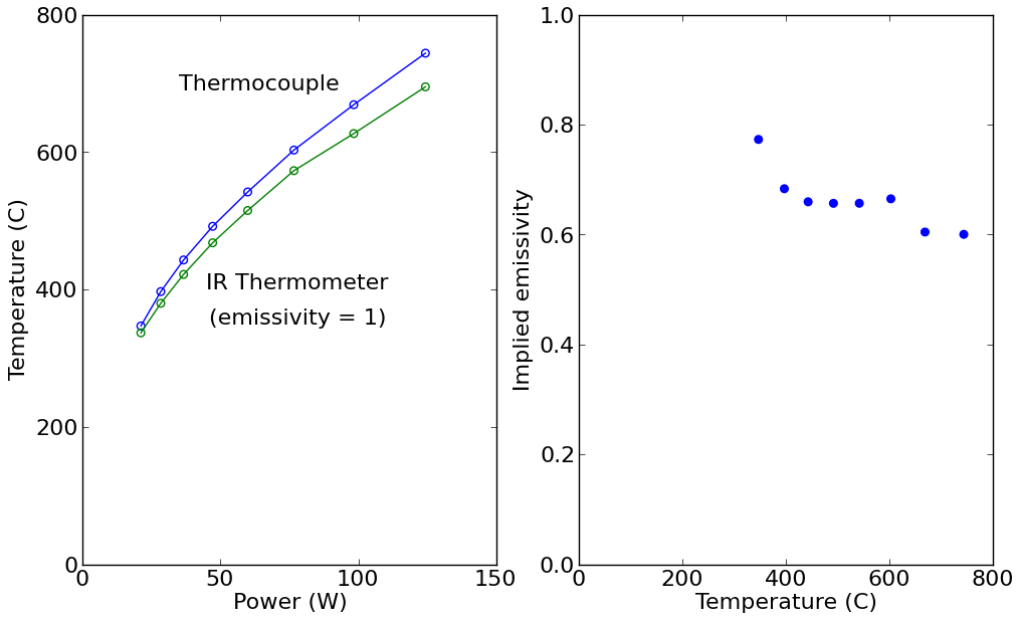

FIGURE 4 (Left) Temperature measured by thermocouple and temperature measured by infrared pyrometer as a function of heater power. (Right) Emissivity calculated from the ratio of the infrared pyrometer measurement to the thermocouple measurement.

measured with the thermocouple. For this device, the measured radiated power is also expressed as a temperature, and we therefore have, in the Wien approximation,

$$\varepsilon_i = \frac{\text{measured power}}{\text{blackbody power}} \propto \frac{\int_{1.0\ \mu m}^{1.6\ \mu m} \frac{2hc^2}{\lambda^5} e^{-\frac{hc}{\lambda k T_m}}\, d\lambda}{\int_{1.0\ \mu m}^{1.6\ \mu m} \frac{2hc^2}{\lambda^5} e^{-\frac{hc}{\lambda k T_b}}\, d\lambda}$$

where T_m is the temperature measured by the iR2, and T_b is the temperature measured by the thermocouple. A more accurate calculation would take into account the shape of the spectral response curve of the detector, but we do not have that information. The integral of the Wien function can be expressed in closed form,

$$\int \frac{2hc^2}{\lambda^5} e^{-\frac{hc}{\lambda kT}}\, d\lambda = -\frac{2}{h^3 c^2} (kT)^4 \left[\left(\frac{hc}{\lambda kT}\right)^3 + 3\left(\frac{hc}{\lambda kT}\right)^2 + 6\frac{hc}{\lambda kT} + 6 \right] e^{-\frac{hc}{\lambda kT}}$$

These equations were used to calculate the implied emissivity values plotted in Figure 4. As can be seen, the values are clustered in the neighborhood of 0.65. Reference values for the emissivity of 300 series stainless steel are in the range of 0.35–0.50 [11]. This is reasonable agreement given that the reference measurements are made on samples with higher quality surface finishes. Other potential causes of the discrepancy are surface oxidation on the heater block and the possibility that reflected light from the heaters is being collected by the optics. The primary cause of the variation in the deduced emissivities is most likely the weakness of the dependence of emissivity on the temperature ratio. In practice, this is an advantage – even if the emissivity is not precisely known, the temperature calculation will still be relatively accurate.

Two-color measurements were also attempted; however, accurate data were not obtained by this method. The iR2 has a "slope" setting to correct for the wavelength dependence of emissivity, but the slope values required to match the optical measurements to the thermocouple measurements were large and inconsistent. A plausible explanation for this effect is again that reflected light from the heaters interfered with the measurement. As described above, the two-color measurements are made by comparing the signal from a silicon detector (shorter wavelength) to that of an InGaAs detector (longer wavelength). Because the heaters are much hotter than the target as a whole, they affect short wavelength measurements more than long wavelength ones.

The expected consequence can be seen by considering an example. If the target surface temperature is 600°C and the heater temperature is 1000°C, the heaters produce 30 times more light at 1550 nm but 140 times more light at 1050 nm. Here, the selected wavelengths are near the long wavelength edge of the detector response, which is appropriate because the blackbody spectrum drops rapidly as the wavelength gets shorter.

3.2 SPECTROMETER

The useful range of the spectrometer was found to be roughly 800–1175 nm. Outside that range, noise severely affected the signal, especially at lower count rates. Because this band is at the short wavelength end of the infrared spectrum, measurements were dominated by reflected light from the heaters. The effect is seen in Figure 5. Here, relative spectra are plotted for various heater power settings. If the only light reaching the instrument were from the target surface, the curves would be much steeper. As an example, at 600°C, the intensity at 1200 nm should be more than a factor of 100 times greater than the intensity at 800 nm. Instead, the curve is relatively flat. Another feature in Figure 5 is that, except for the two lowest target temperatures (347°C and 397°C) , the curves flatten out or dip at the long wavelength end of the spectra. To the lowest order of approximation, this effect is not explained by the presence of reflected light. One potential cause could be errors introduced during collection of the reference spectra. Another is that the spectrum of the lamp used as a reference source could deviate from the

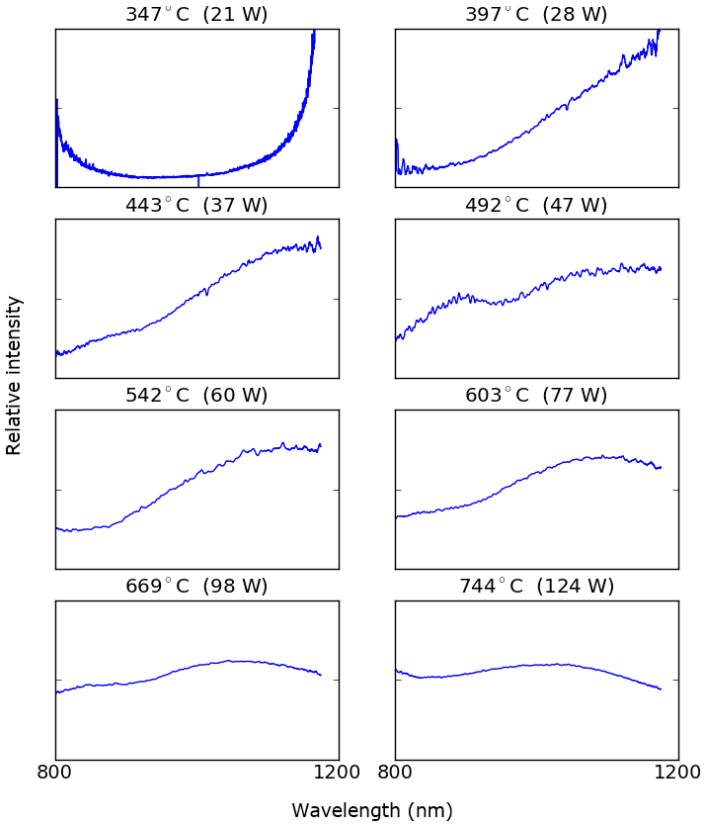

FIGURE 5 Relative infrared spectra versus heater temperature from 347°C to 744°C (measured at the center thermocouple). Radiation reflected from the target heaters eclipsed direct emission from the target. Spectra are normalized to a lamp (approximating a blackbody) at known temperature. Each plot is individually scaled to emphasize the shape of the spectra.

theoretical blackbody spectrum in this wavelength range. The actual cause cannot be established definitively from the available data.

The integration time was set independently at each temperature to minimize the noise while not saturating the detector. For the three lowest heater settings, saturation was not reached at 5 s, the longest possible integration time. The remaining settings were 4 s at 37 W, 1.6 s at 60 W, 800 ms at 77 W, 135 ms at 98 W, and 75 ms at 124 W. Shorter integration times could be achieved, at the expense of wavelength resolution, by replacing the diffraction grating.

4 DISCUSSION

Our tests of temperature measurement with the two instruments have shown that, by looking to a wider range of the spectrum, advantages can be gained in both cost and performance.

The FLIR thermal imaging camera that has been used for target-window temperature measurement in the linac production and thermal experiments described elsewhere operates in the long wavelength part of the infrared spectrum (LWIR). The devices that we have tested here operate in the short wavelength range of the spectrum. The two most common detector materials in this range are silicon and indium gallium arsenide. The sensitivity of silicon falls rapidly past 1 μm to near zero at 1.2 μm. Uncooled InGaAs sensors have high sensitivity to 1.6 μm. Beyond that wavelength, the noise level of uncooled sensors is too high for this application. Cooled sensors, while sensitive at longer wavelengths, are less desirable because they are more complex and costly.

Of the two instruments that were tested, the spectrometer employed a silicon CCD, while the pyrometer used both a silicon detector and an InGaAs detector. However, both types of instruments, as well as area scan sensors such as CCDs, can be based on either of those detector types in addition to other, less frequently used photodetector materials.

Measuring in the near infrared spectrum offers a few immediate advantages: (1) ordinary glass or quartz optical elements can be used; (2) alignment can be performed without heating the target; and (3) emissivity corrections to temperature are typically less than 10%, which is small enough to consider the possibility of disregarding it completely.

If spatial resolution is not required, an infrared pyrometer such as the one used here would be attractive for its low cost and simplicity. The device we purchased cost about $3,500, but less expensive devices with fewer yet sufficient features are available. The required optical design is not challenging, and it could be designed to sample the whole window or a portion of it. In our tests, the two-color mode could not be used because of the experimental configuration, but that issue would not be encountered in practice. The pyrometer is easily aligned by shining a laser beam backwards through the optics onto the target. The lens assembly can be coupled to the electronics with an optical fiber, which allows more flexibility in how the electronics are shielded.

Though not demonstrated here, two-color infrared pyrometers have, in principle, a few benefits over single-color ones. Both single- and two-wavelength measurements are weighted toward the hotter area of the target – a benefit for this application; however, this effect is stronger for two-color measurements. If the emissivity is relatively constant across the wavelength range being observed, two-color measurements do not require the emissivity to be known. This could be a particular advantage if the surface of the window might change gradually over time or abruptly preceding a failure. Additionally, a measurement by the two-color method is not affected if the optical components darken due to radiation exposure, so long as the changes are not wavelength dependent.

For two-color measurements in the temperature range of interest, it would be preferable to use slightly longer wavelengths than the ones used by the instrument we tested. For example, LumaSense advertises a ratio pyrometer that uses 1.28 µm and 1.65 µm (model IGAR 12-LO).

If spatial resolution is required, an area scan detector such as a CCD must be used. The function of CCDs is very similar to that of individual photodetectors, so our analysis is readily extended to cover CCD technology. Both silicon and InGaAs CCDs are available, with silicon CCD cameras costing less than $500, while InGaAs CCD cameras cost between $2000 and $3000. Conventionally, CCDs are illuminated from the front, but back-illuminated CCDs, which have higher sensitivity, are also available. An example calculation for each, specific details of which follow below, is illustrated in Figure 6.

In this example, the camera is assumed to be 4 m from the target, the lens aperture is 25.4 mm, the frame rate is 30 Hz, and the spatial resolution is 1 mm. This spatial resolution could be achieved, for instance, with a 5 µm pixel size (typical for the current generation of silicon CCDs) and a 20 mm lens. It would be possible to increase the resolution at the expense of signal strength. The integrated response was calculated by using a spectral response curve typical of the respective technology. The response of the front-illuminated CCD falls rapidly to zero at about 1100 nm, whereas the back-illuminated CCD extends the range to about 1150 nm. Typical CCDs saturate at 10^5 to 10^6 counts, and while the ability to operate the CCD near saturation is not a requirement, it maximizes the temperature resolution and allows headroom for

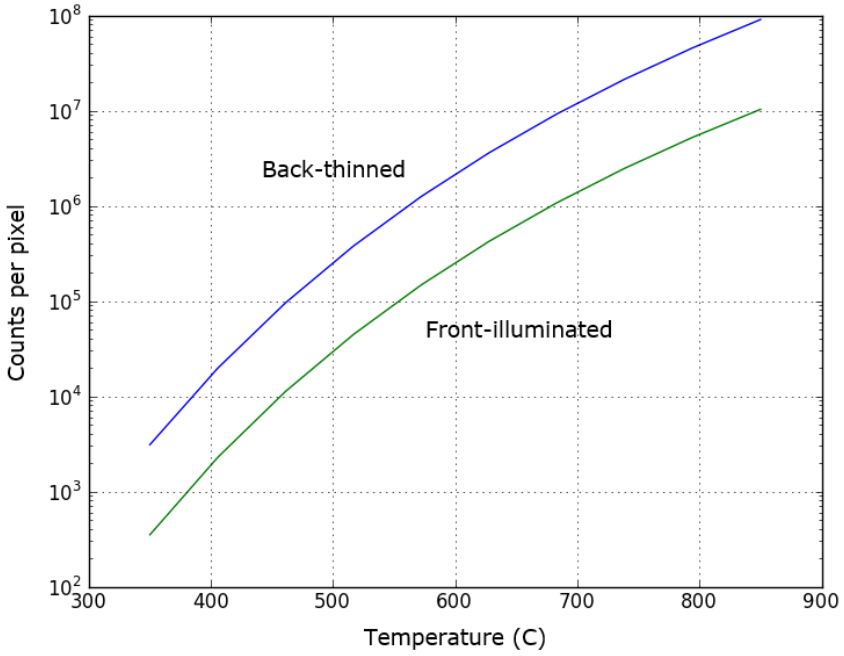

FIGURE 6 Comparison of front-illuminated and back-thinned CCD performance in hypothetical configuration for window temperature monitoring. Assumed frame rate is 30 Hz. Ideally, to measure a given temperature, the number of counts per pixel would exceed 10^5.

inefficiencies in the optical system. Taking 10^5 counts as a figure of merit, a silicon CCD in this configuration saturates in the neighborhood of 500–600°C. At higher temperatures, it would be necessary to insert filters or close down the aperture.

Because of its increased spectral range, InGaAs CCDs would unquestionably perform adequately across this temperature range. They have larger pixels (25 μm is typical), so they would require a different (but still standard) length lens.

At the expense of increased cost and complexity, it would be possible to perform spatially resolved two-color measurements. This would require splitting the image and sending it to two different CCDs. Filters would be used to select different wavelength bands for each detector. Two InGaAs CCDs could be used, or perhaps one silicon CCD and one InGaAs CCD.

5 CONCLUSION

In summary, the primary advantages and disadvantages of each approach are:

Infrared pyrometer, single wavelength
Pros: Simplest implementation; temperature somewhat weighted toward hottest regions
Cons: No spatial resolution

Infrared pyrometer, two wavelength
Pros: Simple; increased weighting toward hot spots; retains accuracy if radiation darkens optics or emissivity of target changes
Cons: No spatial resolution

Silicon CCD
Pros: Low cost; spatial resolution; significant experience in high radiation environments
Cons: Least signal strength headroom

InGaAs CCD
Pros: Spatial resolution; much more headroom compared to silicon
Cons: Higher cost than silicon

Two wavelength CCD
Pros: Combines insensitivity to emissivity changes with spatial resolution
Cons: Cost; complexity

6 REFERENCES

[1] Keith A. Woloshun, "^{100}Mo to ^{99}Mo Production Target Design and Testing Updates," Mo-99 Topical Meeting, Ritz-Carlton, St. Louis, MO, September 11-14, 2016.

[2] Keith A. Woloshun, Gregory E. Dale, Frank P. Romero, and Dale A. Dalmas, "Production Facility Prototype Blower Installation Report with 1000 Hour Test Results," Los Alamos National Laboratory, Los Alamos, NM, Rep. LA-UR-16-22212 (2016).

[3] Keith A. Woloshun, Gregory E. Dale, Eric R. Olivas, and Michal Mocko, "Mo100 to Mo99 Target Cooling Enhancements Report," Los Alamos National Laboratory, Los Alamos, NM, Rep. LA-UR-16-20939 (2016).

[4] Keith A. Woloshun, Gregory E. Dale, Dale A. Dalmas, and Frank P. Romero, "Performance Characterization of the Production Facility Prototype Helium Flow System," Los Alamos National Laboratory, Los Alamos, NM, Rep. LA-UR-15-29563 (2015).

[5] Gregory E. Dale, "Recent Activities at Los Alamos National Laboratory Supporting Domestic Production of 99Mo," Mo-99 Topical Meeting, Ritz-Carlton, St. Louis, MO, September 11-14, 2016.

[6] Sergey D. Chemerisov, "Accelerator-Pathway for ^{99}Mo Production without Highly Enriched Uranium," Mo-99 Topical Meeting, Ritz-Carlton, St. Louis, MO, September 11-14, 2016.

[7] Matt Virgo, Sergey D. Chemerisov, Roman G. Gromov, Charles Jonah, and George F. Vandegrift, "Results of Thermal Test of Metallic Molybdenum Disk Target and Fast Acting Valve Testing," Argonne National Laboratory, Lemont, IL, Rep. ANL/NE-16/44 (2016).

[8] Keith A. Woloshun, Gregory E. Dale, Eric R. Olivas, Frank P. Romero, Dale A. Dalmas, Sergey D. Chemerisov, Roman G. Gromov, and Rick Lowden, "Thermal Test on Target with Pressed Disks," Los Alamos National Laboratory, Los Alamos, NM, Rep. LA-UR-16-22211 (rev. 1), (2016).

[9] Keith A. Woloshun, "Zero Degree Line Mo Target Thermal Test Results and Analysis," Los Alamos National Laboratory, Los Alamos, NM, Rep. LA-UR-15-23134 (2015).

[10] C.C. Davis, *Lasers and Electro-Optics: Fundamentals and Engineering*, Cambridge, UK: Cambridge University Press, pp. 651–606 (1996).

[11] G.C. Holst, *CCD Arrays, Cameras, and Displays*, Winter Park, FL: JCD Publishing (1998).

[12] T.J. Quinn, *Temperature*, 2nd ed., London: Academic Press Limited, pp. 409–422 (1990).

[13] G.G. Gubareff, J.E. Janssen, and R.H. Torborg, *Thermal Radiation Properties Survey: A Review of the Literature*, 2nd ed., Minneapolis, MN: Honeywell Research Center (1960).

[14] A. Rogalski, "Infrared Detectors: An Overview," *Infrared Phys. Techn.*, **43**: 187–209 (2002).

[15] "Omega: Your Source for Process Management and Control," www.omega.com, accessed on March 10, 2016.

[16] "Ocean Optics," oceanoptics.com, accessed on March 10, 2016.

[17] L. Michalski, K. Eckersdorf, J. Kucharski, and J. McGhee, *Temperature Measurement*, West Sussex, England: Wiley, p. 153 (1991).

Nuclear Engineering Division
Argonne National Laboratory
9700 South Cass Avenue, Bldg. 208
Argonne, IL 60439-4854

www.anl.gov